Progress In Electromagnetics Research C, Vol. 99, 99–110, 2020

Early Brain Stroke Detection Using Flexible Monopole Antenna

Md. Ashikur Rahman[1, *], Md. Foisal Hossain[1], Manjurul A. Riheen[2], and Praveen K. Sekhar[2]

Abstract—In this paper, an inkjet printed slotted disc monopole antenna is designed, printed, and analyzed at 2.45 GHz ISM band on a polyethylene terephthalate (PET) substrate for early detection of brain stroke. PET is used as a substrate due to its low loss tangent, flexible, and moisture-resistant properties. By the implementation of slotting method, the size of this antenna is reduced to $40 \times 38\,\text{mm}^2$. The printed antenna exhibits 480 MHz (19.55%) bandwidth ranging from 2.25 GHz to 2.73 GHz frequency. It shows a radiation efficiency of 99% with a realized gain of 2.78 dB at 2.45 GHz frequency. The Monostatic Radar (MR) approach is considered to detect brain stroke by analyzing the variations in received signals from the head model with and without stroke. The maximum specific absorption rate (SAR) distribution at 2.45 GHz frequency is calculated. The compact size and flexible properties make this monopole antenna suitable for early detection of brain stroke.

1. INTRODUCTION

Statistics categorizes stroke as the second most common reason for death [1] and the third most reason for disability [2]. If the treatment is ensured faster for stroke patients, the possibilities of recovery are higher. The traditional brain stroke detection techniques are Computed Tomography (CT), Positron Emission Tomography (PET), Magnetic Resonance Imaging (MRI), Electroencephalography (EEG), Magneto-encephalography (MEG), Magnetic Induction Tomography (MIT), and Electrical Impedance Tomography (EIT) [3]. An alternative screening technique which can be administered bedside or in an ambulance is necessary for point of care detection and early screening [4]. Paramedics can provide crucial information about the patient's symptoms and the test results to the hospital on the route. Brain stroke detection using Electromagnetic Impedance Tomography (EMIT, a non-invasive medical imaging technique using microwave devices) is gaining significant momentum as a surrogate technique to the state-of the art screening techniques.

In EMIT based brain stroke detection scheme, antenna plays a crucial role. In literature, different EMIT based stroke detection techniques can be found which use rigid and flexible antennas [3–10]. The free space performance of these antennas is presented in Table 1. Munawar et al. utilized EMIT technique using microwave signals to detect stroke [3]. Mobashsher et al. [5] used a 3D wideband unidirectional antenna with an overall dimension of $70 \times 60 \times 15\,\text{mm}^3$ designed on 1.52-mm-thick GIL GML 1032 substrates to detect the stroke. They presented a technique based on the contrast of reflection phases for stroke detection collecting scattered signals from the antennas and investigating them to reduce the strain of the system. Mohammed et al. used variations in the reflection coefficients to detect stroke using an array of eight tapered slot antennas (TSA), each with dimensions of $24 \times 24 \times 0.62\,\text{mm}^3$ on a Rogers RT6010 substrate [6]. Wu and Pan used directional folded antennas with a dimension of $81.2 \times 80 \times 1.6\,\text{mm}^3$, each on an FR-4 substrate to detect stroke [7]. They classified the results from the human brain model simulation by algorithms, such as PCA and LDA classification algorithms to verify the efficacy of the antenna and found accurate classification.

Received 7 December 2019, Accepted 22 January 2020, Scheduled 30 January 2020

* Corresponding author: Md. Ashikur Rahman (ashikur.rahman0809@gmail.com).

[1] Department of Electronics and Communication Engineering, Khulna University of Engineering & Technology, Khulna-9203, Bangladesh. [2] School of Engineering and Computer Science, Washington State University, Vancouver, WA, USA.

Table 1. Literature summary of the performance of antennas used for brain stroke detection.

References	Size (mm^2)	Substrate	Thickness (mm)	Bandwidth	Peak Gain
Mobashsher et al. [5]	70×60	GIL GML 1032	1.52	1.52 GHz (77%)	5 dBi
Wu et al. [7]	81×80	FR-4	1.6	1.36 GHz (76%)	4.5 dBi
Jamlos et al. [8]	80×45	Taconic (TLY-5)	1.57	10.6 GHz (133.76%)	12.12 dB
Bashri et al. [9]	70×30	PET	0.075	2.2 GHz (91.67%)	*
Alqadami et al. [10]	85×60	PDMS Polymer	2.5	0.78 GHz (50.32%)	3.5 dBi

* Not Available

Jamlos et al. detected stroke with an ultra-wideband antenna with a dimension of $80 \times 45 \times 1.57\,mm^3$ designed on a Taconic (TLY-5) substrate [8]. The authors used the Inverse Fast Fourier Transform (IFFT) for easier analysis of S-parameters and smoothing '*mslowess*' procedure to filter out the noise for accurate results. Using an array of 8 antennae with a dimension of $70 \times 30\,mm^2$, each printed on a 75-µm-thick PET substrate, Bashri et al. investigated a wearable head imaging system [9]. Alqadami et al. used a flexible and wideband 8-element array antenna with a dimension of $85 \times 60 \times 4\,mm^3$ based on a multilayer PDMS polymer substrate to detect brain stroke with a head imaging system [10]. Above discussed investigations take time for effective image reconstruction [11] and have strong multipath reflections due to array configuration [12, 13]. All these techniques used rigid substrates except Bashri et al. [9] and Alqadami et al. [10]. Though Bashri et al. and Alqadami et al. used flexible substrates, these antennas have comparatively larger dimensions due to the array configuration. Current research on EMIT based stroke detection is focusing on antennas that are compact and conformal to improve the resolution and accuracy of the results.

In this paper, a compact slotted disc monopole antenna is designed and printed on a PET substrate for early detection of brain stroke. The size of this antenna is reduced to $40 \times 38\,mm^2$ as compared to earlier reported antennas for stroke detection [5, 7–10]. Silver nanoparticles (AgNPs) ink is used due to its high conductivity (6.3×10^7 S/m) [14] and anti-oxidation properties unlike copper nanoparticles (CuNPs) ink which is extremely vulnerable to oxidation in the air [15]. PET substrate is preferred to other flexible substrates such as photo paper due to its low loss tangent and moisture resistant properties. The Monostatic Radar (MR) approach is considered to detect brain stroke due to its simplicity. Also, the SAR distributions of this antenna are calculated at 2.45 GHz frequency for a maximum power level of 20 dBm in CST Microwave Studio.

2. ANTENNA AND HUMAN HEAD PHANTOM MODEL DESIGN

2.1. Antenna Geometry

The overall dimension of the antenna is $40 \times 38 \times 0.135\,mm^3$ printed on a PET substrate with commercially available silver nanoparticles ink provided by NovaCentrix. This PET substrate possesses a relative permittivity, $\varepsilon_r = 3.2$, with loss tangent, $\tan\delta = 0.022$. A coplanar waveguide (CPW) feed technique is used. A SMA (Sub-miniature version A) connector is connected with the CPW feeding line using conducting paste. The optimized values of geometric variables simulated in CST Microwave Studio are listed in Table 2. The evolution of the structure of the proposed antenna is shown in Figure 1. Design I is shown in Figure 1(a). A pentagonal slot with a radius, R_P (mm), is added inside a circular disc in Design II shown in Figure 1(b) which is crucial for the expected resonant frequency. Design II is the proposed antenna with a circular disc having a radius of 16.75 mm with a pentagonal slot. The return loss graphs of Design I and Design II (proposed) are shown in Figure 2. In Design I, (for a circular disc of radius R mm) the -10 dB return loss level starts at around 2.6 GHz and resonates at around 3.5 GHz with a minimum return loss around -22 dB. A pentagonal slot is added to Design I to optimize the resonant frequency at 2.45 GHz, resulting in a -29 dB return loss and a bandwidth around 550 MHz (2.22–2.77 GHz).

Table 2. Optimized variables of the proposed antenna.

Variable Name	Symbol	Unit (mm)
Width of substrate	W	38
Length of substrate	L	40
Width of the feeding line	W_F	2.32
Gap between feeding line and ground	G_F	0.3
Thickness of PET substrate	H	0.135
Length of feeding line	L_F	5.5
Radius of circular disc	R	16.75
Length of one side ground plane	L_G	4.50
Width of one side ground plane	W_G	17.54
Radius of pentagonal slot	R_P	16.5

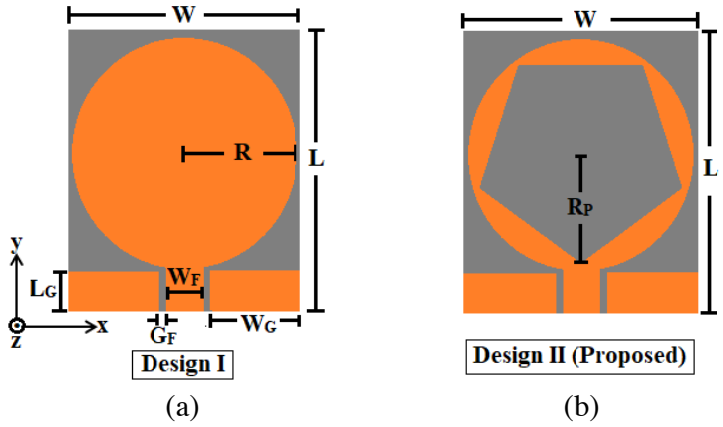

Figure 1. Evolution of the proposed antenna (a) Design I; (b) Design II (Proposed).

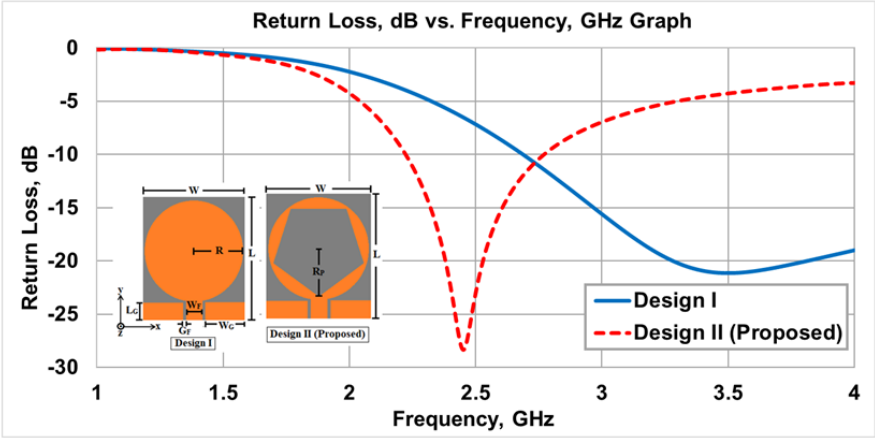

Figure 2. S-parameter plot of the antenna Design I and Design II (proposed).

2.2. Human Head Phantom Model and Stroke Model

The wearable antennas require a detailed analysis of the interaction of the antenna with the human body. A 7-layer human head model and single layer stroke model are designed and analyzed for 2.45 GHz

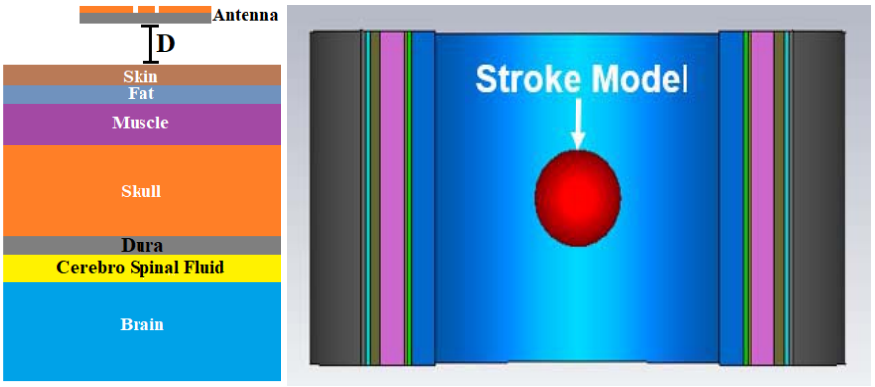

Figure 3. (a) 7-layer human head model with the proposed antenna; (b) single-layer spherical stroke model.

frequency in this section. The head model including layers of skin (dry), fat, muscle, skull, dura, cerebro-spinal fluid, and brain is shown in Figure 3(a). The proposed antenna is placed at a distance of D (mm) that denotes the separation distance of the proposed antenna with the human head model. The electrical properties such as permittivity (ε_r) and conductivity (σ) of the 7-layer model along with the thickness of skin (dry), fat, muscle, skull, dura, cerebro-spinal fluid, and brain respectively are listed in Table 3. The single-layer stroke model is considered to be a spherical blood clot with a 15 mm radius shown in Figure 3(b). The values of the body tissue dielectric parameters are computed using a 4-Cole-Cole Model [16].

Table 3. Dielectric parameters of the 7-layer human head phantom model and stroke model at 2.45 GHz.

Frequency (MHz)	Head Layers	Thickness (mm)	Permittivity, ε	Conductivity, σ (S/m^2)
2450	Skin (Dry)	2	38.006660	1.464073
	Fat	2	5.280096	0.104517
	Muscle	4	53.573540	1.810395
	Skull	10	14.965101	0.599694
	Dura	1	42.035004	1.668706
	Cerebro Spinal Fluid	2	66.243279	3.457850
	Brain	10	42.538925	1.511336
	Stroke Model — blood	Radius, $R_S = 15$	58.263756	2.544997

2.3. Antenna Fabrication

The designed monopole antenna is fabricated on a PET substrate in a Fujifilm Dimatix 2831 Inkjet Printer (DMP) in which 10 pL and 1 pL volume cartridges are available for precise printing. In this experiment, 10 pL cartridge is used having 16 nozzles of 21 µm. Silver nanoparticles ink is used with specifications Ag content 40 wt%, viscosity 8 to 12 cp, and surface tension of 19–30 dyne/cm in order to optimize the properties of inkjet printing. PET substrate-based printed patterns with high conductivity are reported in an earlier study [17] by the authors, and the optimized inkjet printing parameters are used in this study. Using an Agilent PNA-LN5230C vector network analyzer (VNA), the simulated results are verified. Figure 4(a) shows the fabricated antenna with SMA connector, while Figure 4(b) shows the bending structure of the printed antenna. The antenna is then attached to an SMA connector

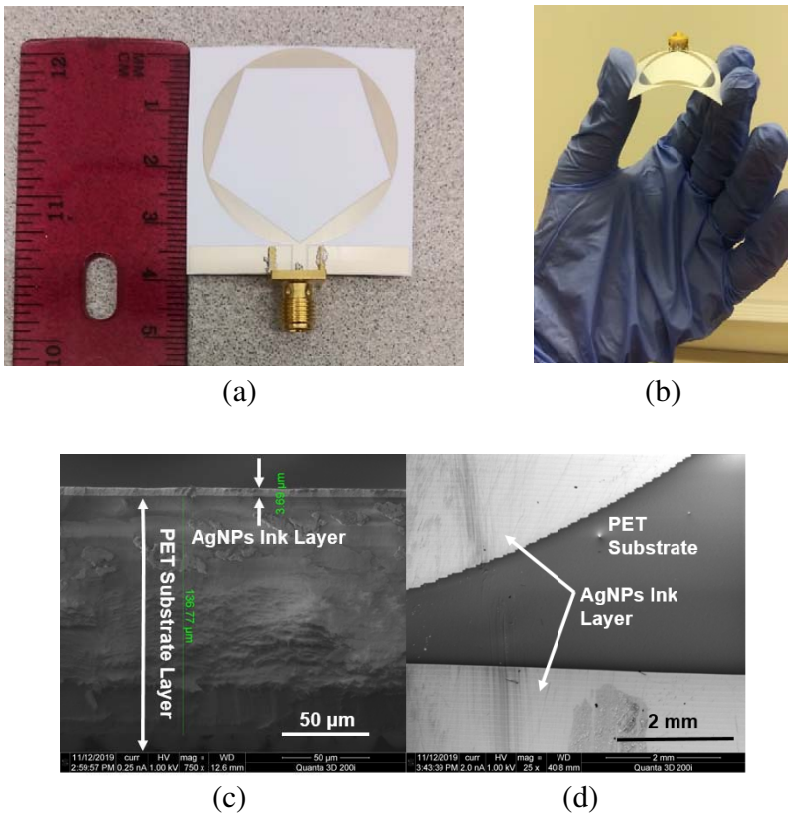

Figure 4. Fabrication of the antenna: (a) photograph of the printed antenna; (b) bending structure of printed antenna; (c) cross-section SEM image of the printed antenna; (d) SEM image of the printed antenna indicating sharp edges.

using a conductive paste. The cross-section Scanning Electron Microscope (SEM) images of the printed antenna are shown in Figure 4(c). The good contact between the ink and the substrate can be observed. The thickness of the silver nanoparticles ink (AgNPs) ink layer found in the SEM is about 3.7 µm which is sufficient to sustain during bending of the antenna. Figure 4(d) shows the uniform silver ink distribution on the PET substrate along with sharp edges.

3. RESULTS AND DISCUSSION

The measured return loss (dB) of the printed antenna is about −20 dB at 2.45 GHz. It exhibits a −10 dB return loss bandwidth of around 480 MHz (2.24–2.72 GHz). Figure 5(a) shows the simulated and measured *s*-parameter graph. It can be inferred from the graph that the measured result shows good agreement with the simulation one. Figure 5(b) shows the printed antenna measurement setup with an Agilent PNA-LN5230C vector network analyzer (VNA). In the literature, experimental results of CPW-fed monopole antennas on a PET substrate are presented and analyzed. Table 4 shows the comparison among the proposed antenna and other CPW-fed monopole antennas on the PET substrate presented in the literature.

Antenna radiation patterns simulated for flat and bent conditions in co-polarization and cross-polarization for $\varphi = 0^\circ$ and $\varphi = 90^\circ$ respectively are shown in Figure 6. Radiation patterns of flat and bent antennas show omnidirectional radiation pattern in both co-polarization and cross-polarization directions. The proposed antenna shows an efficiency of 99% in a flat position when being simulated in free space. Figure 7(a) shows the efficiency graph for flat and bent positions. The proposed antenna has a peak gain of 2.78 dB at 2.45 GHz in free space at the flat position. The gain plot of the antenna in the flat and bent positions is shown in Figure 7(b).

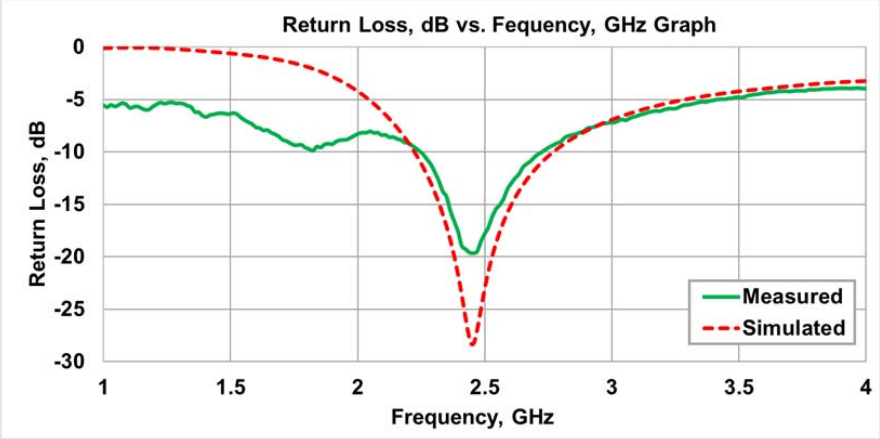

(a)

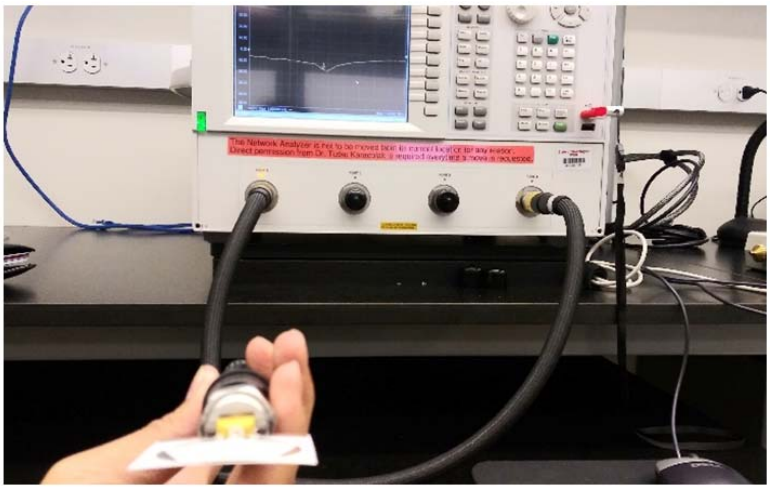

(b)

Figure 5. *S*-parameter plot of the antenna: (a) simulated and measured; (b) measurement with an Agilent PNA-LN5230C vector network analyzer (VNA).

In flexible and wearable antennas, it is essential to consider bending for in-vitro applications. Resonant frequency and return loss are prone to be shifting or deteriorating as a result of variation in the effective length of the designed antenna elements and due to mismatch of the impedance. Figure 8 shows the variation of return loss graph for flat and bent antennas. It can be realized from the graph that the antenna still operates in the ISM band after bending.

In this section, a portable Monostatic Radar (MR) based system is described for the early detection of brain stroke. Figure 9 shows a portable mono-static radar system for scanning the human head. In this system, the compact antenna plays a significant role as it acts as a transceiver antenna to transmit a signal and receive the scattered signal from an abnormal human head. To acquire the data quickly, a microwave transceiver is used, which is compact. Later, the signal processing algorithms are used, which can visualize the received signal variation due to the brain stroke inside the human head analyzing the received signals to form a digital image using digital image processing algorithms.

Two antenna arrangement scenarios, with stroke and without stroke, are set up for simulation in CST Microwave Studio, as shown in Figure 10. Figure 11 shows the variation in reflected time signals obtained from the simulation of the two antenna arrangements for without stroke and with stroke. It is seen from this graph that the reflected signal of the antenna arrangement with stroke shows a slightly higher magnitude than that of the antenna arrangement without stroke. The measure of the difference in reflected signals can be significantly improved by the utilization of an antenna array. In real time

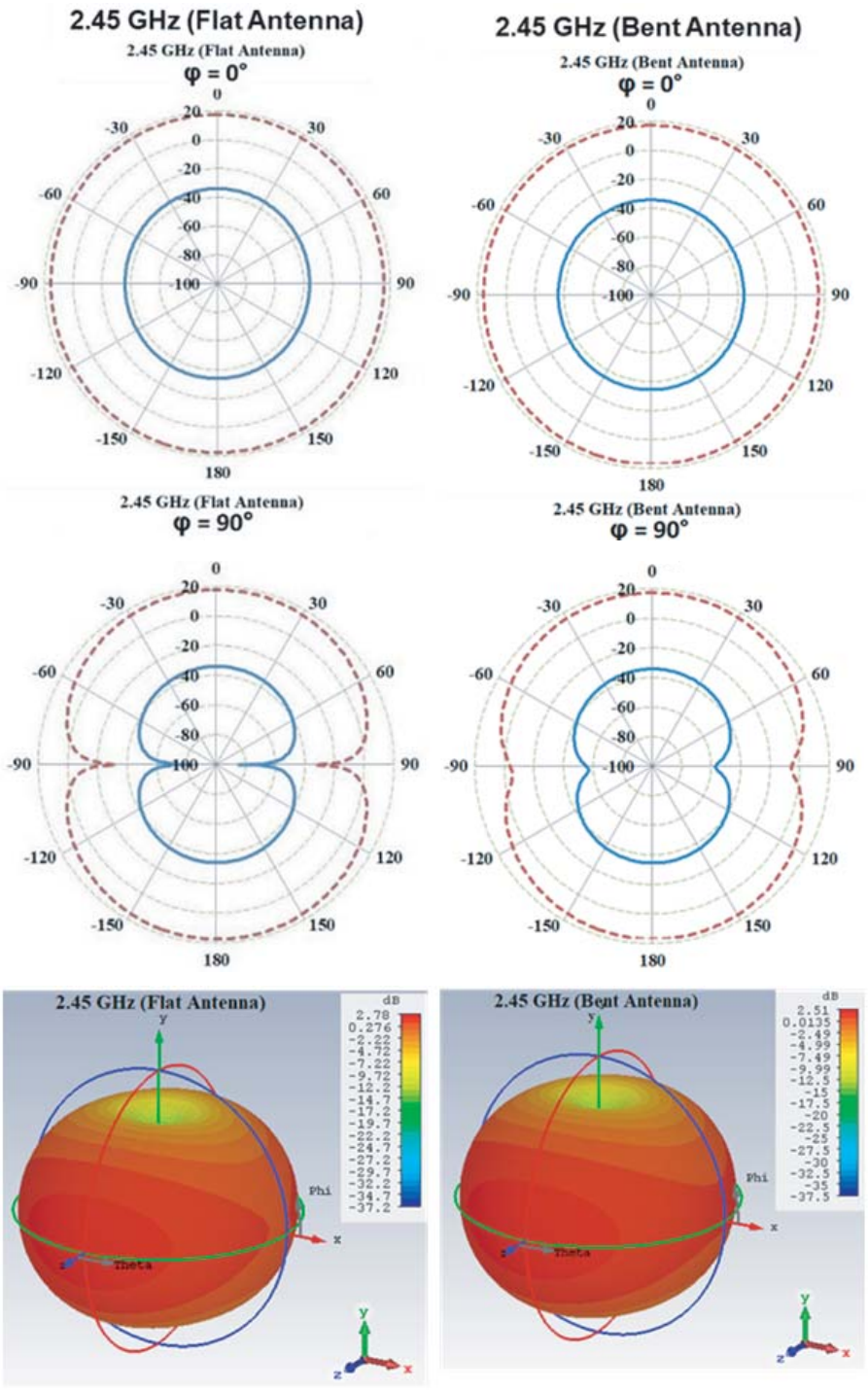

Figure 6. Simulated radiation patterns of the PET-based monopole antenna at 2.45 GHz. The red-colored dotted graphs are for co-polarization (CP), and blue-colored graphs are cross-polarization (XP).

field conditions, an antenna array will be set around the head, and reflected signals will be collated and processed by digital signal processing algorithms. The collated signals can then be visualized as a 2D image using digital image processing algorithms [23, 24]. This antenna might be a basis for a futuristic diagnostic tool for point-of-care stroke detection by the first responders.

Specific Absorption Rate (SAR) is the calculation of power take-up by the body tissues when being

Table 4. Comparison with other CPW-fed monopole antennas on PET substrate presented in the literature.

References	Antenna Size (mm^2)	Substrate Thickness (μm)	Bandwidth	Peak Directive Gain
Guo et al. [18]	40 × 35	300	530 MHz (20.87%)*	**
Hasan et al. [19]	86.9 × 54.7	50	280 MHz (11.66%)	16.24 dBi
Paracha et al. [20]	71 × 49	125	300 MHz (12.24%)	1.44 dBi
Saeed et al. [21]	59 × 31	100	160 MHz (6.6%)	1 dBi
Bait-Suwailam & Alomainy [22]	45 × 40	135	770 MHz (34%)	1.81 dBi
Bashri et al. [9]	70 × 30	75	2.2 GHz (91.67%)	**
This work	40 × 38	135	480 MHz (19.55%)	2.8 dBi

* Approximated
** Not Available

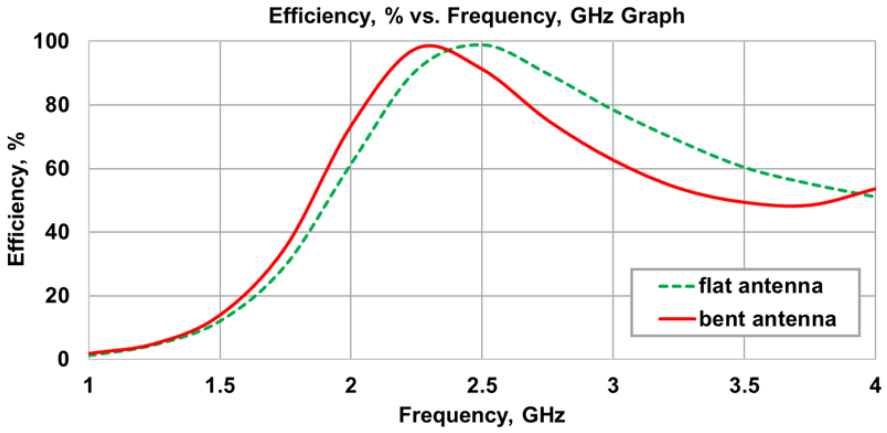

(a)

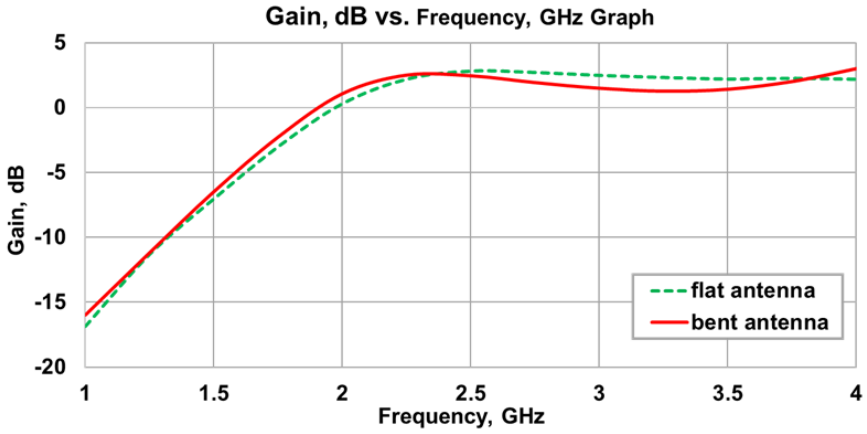

(b)

Figure 7. Antenna efficiency and gain graph: (a) efficiency graph (at flat and bend condition); (b) gain graph (at flat and bend condition).

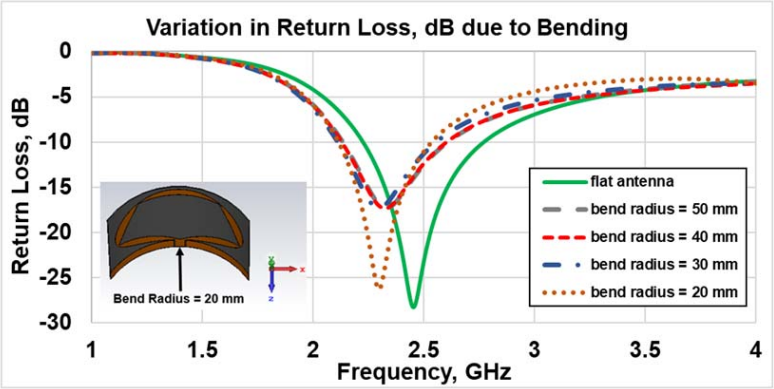

Figure 8. Variation in return loss graph due to bending.

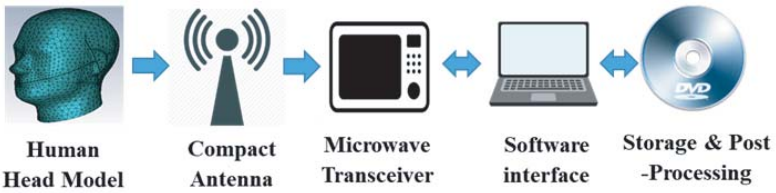

Figure 9. A portable monostatic radar system.

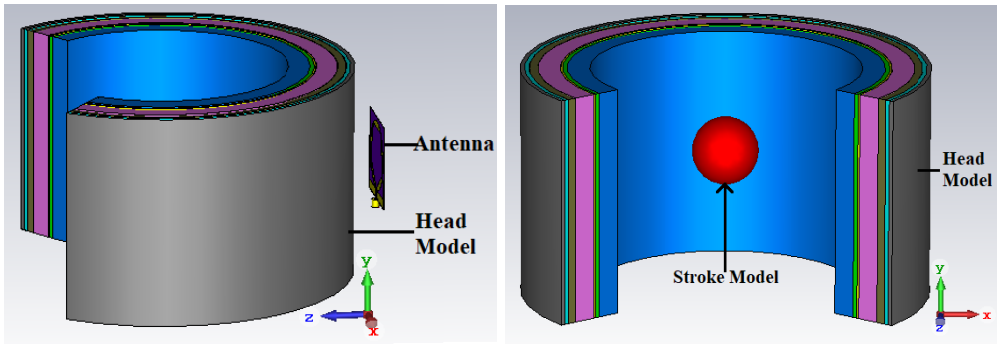

(a) (b)

Figure 10. Antenna arrangement with the 7-layer human head model: (a) without stroke; (b) with stroke.

open to radio frequency (RF) electromagnetic waves. The effects of antenna radiation on the human body must be quantified for wearable applications due to ensuring the safety of the human body open to the electromagnetic radiation. Excessive exposure beyond safety limits can be injurious to human health. The following equation is used for calculating SAR:

$$\text{SAR} = \frac{\sigma * |E|^2}{\rho} \tag{1}$$

where σ denotes the conductivity of the tissue, E the electric field, and ρ the mass density of the tissue. In vitro SAR calculation is carried out in this section with a 7-layer cylindrical human head model of a 90 mm cylindrical radius and the antenna. A separation distance of 1 cm between the human head model and the proposed antenna is considered for the measurement of the SAR. Figure 12 shows the SAR distribution patterns of the antenna at 2.45 GHz frequency. The simulated results show that the

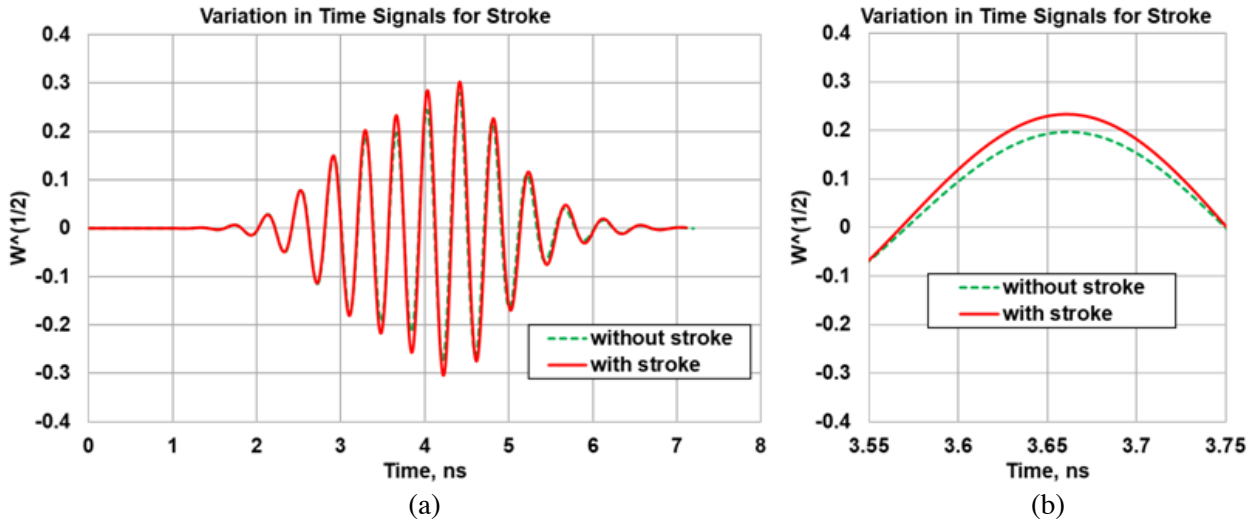

Figure 11. Variation in reflected time signals: (a) without stroke and with stroke; (b) difference in reflected time signals (zoomed).

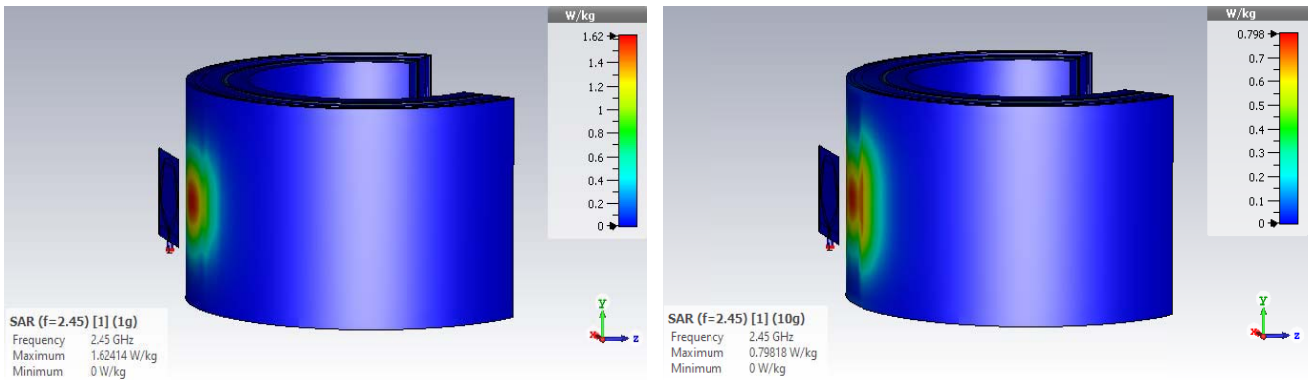

Figure 12. Distribution of SAR averaged over; (a) 1 g of tissue; (b) 10 g of tissues.

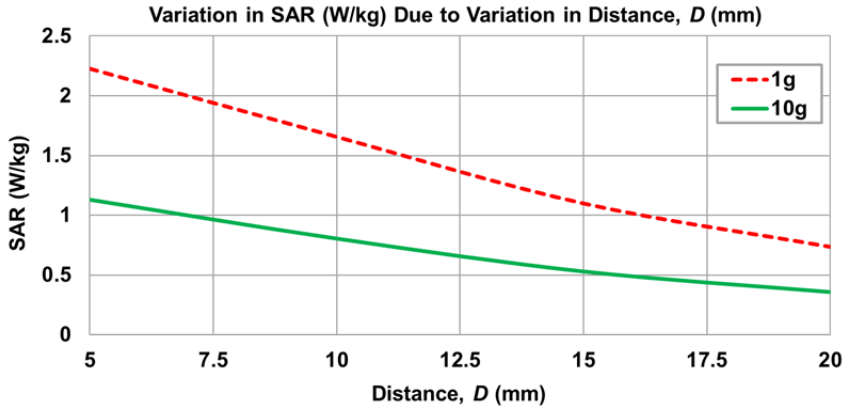

Figure 13. Variation in SAR (W/kg) due to the separation distance between the head model and antenna.

calculated values for 1 g and 10 g of tissues are 1.61 W/kg and 0.8 W/kg respectively which follow the standard limits defined by ICNIRP [25] and IEEE [26] for a maximum input power of 100 mW. Variation in the graph of SAR values due to the variation in distance of the antenna with the human head is shown in Figure 13. It is evident from the graph that with an increase in distance of the placement of the antenna, the SAR values decrease and vice versa. It is recommended to use this antenna at a minimum distance of 1 cm from the head to maintain safety limits and also to maintain acceptable antenna performance for a maximum input power of 20 dBm at 2.45 GHz frequency.

4. CONCLUSIONS

In this paper, an inkjet-printed slotted disc monopole antenna on a PET substrate is presented for early brain stroke detection application. This printed antenna exhibits a bandwidth of 480 MHz (19.55%), along with a realized gain of 2.78 dB. The performance of this antenna is adequate in bent and cylindrical head proximity conditions for ISM band applications. Also, the SAR distribution shows that the values are well within the safety limits. This study serves as a proof of concept validation of stroke detection by EMIT technique. With sufficient controls in place and in-depth study of various critical factors such as temperature and pulse of the patient, a point of care device could come into fruition. The magnitude of the variation in reflected signals can be significantly enhanced by using the antenna array. In the future, an antenna array will be placed on the head, and reflected signals will be collated and processed by digital signal processing algorithms. The signature can then be visualized as a 2D image using digital image processing algorithms. This antenna might be a basis for a futuristic diagnostic tool for point-of-care stroke detection by the first responders. The flexible and compact nature of this printed monopole antenna enables the feasibility of a future surrogate device for early brain stroke detection.

REFERENCES

1. Lozano, R., et al., "Global and regional mortality from 235 causes of death for 20 age groups in 1990 and 2010: A systematic analysis for the Global Burden of Disease Study 2010," *The Lancet*, Vol. 380, No. 9859, 2095–2128, 2012.
2. Murray, C. J., et al., "Disability-adjusted life years (DALYs) for 291 diseases and injuries in 21 regions, 1990–2010: A systematic analysis for the Global Burden of Disease Study 2010," *The Lancet*, Vol. 380, No. 9859, 2197–2223, 2012.
3. Munawar Qureshi, A., Z. Mustansar, and A. Maqsood, "Analysis of microwave scattering from a realistic human head model for brain stroke detection using electromagnetic impedance tomography," *Progress In Electromagnetics Research M*, Vol. 52, 45–56, 2016.
4. Mobashsher, A. T., K. Bialkowski, A. Abbosh, and S. Crozier, "Design and experimental evaluation of a non-invasive microwave head imaging system for intracranial haemorrhage detection," *Plos One*, Vol. 11, No. 4, e0152351, 2016.
5. Mobashsher, A., B. Mohammed, A. Abbosh, and S. Mustafa, "Detection and differentiation of brain strokes by comparing the reflection phases with wideband unidirectional antennas," *2013 International Conference on Electromagnetics in Advanced Applications (ICEAA)*, 1283–1285, IEEE, 2013.
6. Mohammed, B., A. Abbosh, and D. Ireland, "Stroke detection based on variations in reflection coefficients of wideband antennas," *Proceedings of the 2012 IEEE International Symposium on Antennas and Propagation*, 1–2, 2012, IEEE.
7. Wu, Y. and D. Pan, "Directional folded antenna for brain stroke detection based on classification algorithm," *2018 IEEE 4th Information Technology and Mechatronics Engineering Conference (ITOEC)*, 499–503, IEEE, 2018.
8. Jamlos, M., M. Jamlos, and A. Ismail, "High performance novel UWB array antenna for brain tumor detection via scattering parameters in microwave imaging simulation system," *2015 9th European Conference on Antennas and Propagation (EuCAP)*, 1–5, IEEE, 2015.

9. Bashri, M. S. R., T. Arslan, and W. Zhou, "Flexible antenna array for wearable head imaging system," *2017 11th European Conference on Antennas and Propagation (EUCAP)*, 172–176, IEEE, 2017.
10. Alqadami, A. S., K. S. Bialkowski, A. T. Mobashsher, and A. M. Abbosh, "Wearable electromagnetic head imaging system using flexible wideband antenna array based on polymer technology for brain stroke diagnosis," *IEEE Transactions on Biomedical Circuits and Systems*, Vol. 13, No. 1, 124–134, 2018.
11. Mahmood, Q., et al., "A comparative study of automated segmentation methods for use in a microwave tomography system for imaging intracerebral hemorrhage in stroke patients," *Journal of Electromagnetic Analysis and Applications*, Vol. 7, No. 05, 152, 2015.
12. Meaney, P. M., F. Shubitidze, M. W. Fanning, M. Kmiec, N. R. Epstein, and K. D. Paulsen, "Surface wave multipath signals in near-field microwave imaging," *Journal of Biomedical Imaging*, Vol. 2012, 8, 2012.
13. Bourqui, J., J. Garrett, and E. Fear, "Measurement and analysis of microwave frequency signals transmitted through the breast," *Journal of Biomedical Imaging*, Vol. 2012, 1, 2012.
14. Naghdi, S., K. Y. Rhee, D. Hui, and S. J. Park, "A review of conductive metal nanomaterials as conductive, transparent, and flexible coatings, thin films, and conductive fillers: Different deposition methods and applications," *Coatings*, Vol. 8, No. 8, 278, 2018.
15. Dabera, G. D. M., M. Walker, A. M. Sanchez, H. J. Pereira, R. Beanland, and R. A. Hatton, "Retarding oxidation of copper nanoparticles without electrical isolation and the size dependence of work function," *Nature Communications*, Vol. 8, No. 1, 1894, 2017.
16. Gabriel, C., "Compilation of the dielectric properties of body tissues at RF and microwave frequencies," Dept. of Physics, King'S Coll London (United Kingdom), 1996.
17. Riheen, M. A., T. K. Saha, and P. K. Sekhar, "Inkjet printing on PET substrate," *Journal of the Electrochemical Society*, Vol. 166, No. 9, B3036–B3039, 2019.
18. Guo, X., Y. Hang, Z. Xie, C. Wu, L. Gao, and C. Liu, "Flexible and wearable 2.45 GHz CPW-fed antenna using inkjet-printing of silver nanoparticles on pet substrate," *Microwave and Optical Technology Letters*, Vol. 59, No. 1, 204–208, 2017.
19. Hassan, A., S. Ali, G. Hassan, J. Bae, and C. H. Lee, "Inkjet-printed antenna on thin PET substrate for dual band Wi-Fi communications," *Microsystem Technologies*, Vol. 23, No. 8, 3701–3709, 2017.
20. Paracha, K. N., S. K. A. Rahim, H. T. Chattha, S. S. Aljaafreh, and Y. C. Lo, "Low-cost printed flexible antenna by using an office printer for conformal applications," *International Journal of Antennas and Propagation*, Vol. 2018, 2018.
21. Saeed, S. M., C. A. Balanis, and C. R. Birtcher, "Inkjet-printed flexible reconfigurable antenna for conformal WLAN/WiMAX wireless devices," *IEEE Antennas and Wireless Propagation Letters*, Vol. 15, 1979–1982, 2016.
22. Bait-Suwailam, M. M. and A. Alomainy, "Flexible analytical curve-based dual-band antenna for wireless body area networks," *Progress In Electromagnetics Research*, Vol. 84, 73–84, 2019.
23. Islam, M., M. Mahmud, M. T. Islam, S. Kibria, and M. Samsuzzaman, "A low cost and portable microwave imaging system for breast tumor detection using uwb directional antenna array," *Scientific Reports*, Vol. 9, No. 1, 1–13, 2019.
24. Mohammed, B., D. Ireland, and A. Abbosh, "Experimental investigations into detection of breast tumour using microwave system with planar array," *IET Microwaves, Antennas & Propagation*, Vol. 6, No. 12, 1311–1317, 2012.
25. Guideline, I., "Guidelines for limiting exposure to time-varying electric, magnetic, and electromagnetic fields (up to 300 GHz)," *Health Phys.*, Vol. 74, No. 4, 494–522, 1998.
26. IEEE C95.1-2019, "IEEE standard for safety levels with respect to human exposure to electric, magnetic, and electromagnetic fields, 0 Hz to 300 GHz," IEEE, 2019, [Online]. Available: https://standards.ieee.org/standard/C95_1-2019.html#Standard.